JACS
JOURNAL OF THE AMERICAN CHEMICAL SOCIETY
Article
pubs.acs.org/JACS

Tunable Organic Photocatalysts for Visible-Light-Driven Hydrogen Evolution

Reiner Sebastian Sprick,[†] Jia-Xing Jiang,[†,‡] Baltasar Bonillo,[†] Shijie Ren,[†,§] Thanchanok Ratvijitvech,[†] Pierre Guiglion,[∥] Martijn A. Zwijnenburg,[∥] Dave J. Adams,*[,†] and Andrew I. Cooper*[,†]

[†]Department of Chemistry and Centre for Materials Discovery, The University of Liverpool, Crown Street, Liverpool L69 7ZD, United Kingdom

[‡]School of Materials Science & Engineering, Shaanxi Normal University, Xi'an 710062, PR China

[§]College of Polymer Science and Engineering, Sichuan University, Chengdu 610065, PR China

[∥]Department of Chemistry, University College London, 20 Gordon Street, London WC1H 0AJ, United Kingdom

Supporting Information

ABSTRACT: Photocatalytic hydrogen production from water offers an abundant, clean fuel source, but it is challenging to produce photocatalysts that use the solar spectrum effectively. Many hydrogen-evolving photocatalysts are active in the ultraviolet range, but ultraviolet light accounts for only 3% of the energy available in the solar spectrum at ground level. Solid-state crystalline photocatalysts have light absorption profiles that are a discrete function of their crystalline phase and that are not always tunable. Here, we prepare a series of amorphous, microporous organic polymers with exquisite synthetic control over the optical gap in the range 1.94−2.95 eV. Specific monomer compositions give polymers that are robust and effective photocatalysts for the evolution of hydrogen from water in the presence of a sacrificial electron donor, without the apparent need for an added metal cocatalyst. Remarkably, unlike other organic systems, the best performing polymer is only photoactive under visible rather than ultraviolet irradiation.

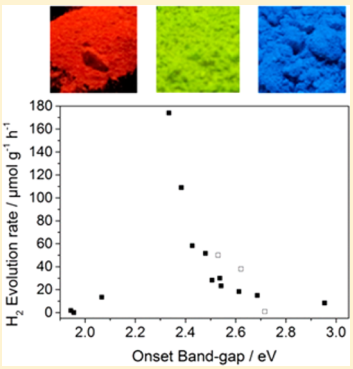

INTRODUCTION

Many studies have focused on inorganic semiconductors as photocatalysts for hydrogen production from water using ultraviolet (UV) or visible light.[1−3] Organic semiconductors are much less explored, but they are intriguing because of their diverse synthetic modularity, which allows their electronic and structural properties to be tailored. Conjugated linear poly(*p*-phenylene)s[4,5] can catalyze hydrogen evolution, but they are only modestly active under UV irradiation and their performance under visible light is very poor. In 2009, Antonietti and co-workers reported an organic photocatalyst for hydrogen evolution based on graphitic carbon nitride (g-C_3N_4).[6] The quantity of hydrogen evolved for native g-C_3N_4 was low, but this was significantly improved upon addition of platinum as a cocatalyst. Copolymerization routes to carbon nitrides were shown to dramatically increase the rate of hydrogen production, again using platinum as a cocatalyst.[7−9] Carbon nitrides are visible light photocatalysts; like polyphenylenes, however, they are most active in UV light.[6,9] Microstructure appears to influence activity in carbon nitrides: for example, mesoporosity was shown to significantly increase the amount of hydrogen evolved.[10,11] Related organic polymers, such as a poly(triazine imide) doped with 4-amino-2,6-dihydroxypyrimidine[12] and a heptazine-based network,[13] are also effective photocatalysts for hydrogen evolution. In all of these cases, platinum was added as a cocatalyst in combination with a sacrificial electron donor. Other modifiers can be used: for example, Ag_2S-modified[14] and polypyrrole-modified[15] carbon nitrides were recently reported. The rates of hydrogen evolution for these organic solids are lower than for some inorganic photocatalysts, but improved rates can be achieved by using liquid-assisted grinding approaches[16] or sol−gel syntheses[17] or by controlling the degree of polymerization and the proton concentration.[18]

Other than carbon nitrides and linear poly(*p*-phenylene)s, there are few examples of organic polymers that act as photocatalysts for hydrogen evolution from water. A small number of nitrogen-containing polymers have been studied, such as poly(azomethines),[19] where the optical gap could be tuned to some extent by the choice of monomer. Likewise, a hydrazone-based covalent organic framework showed significant hydrogen evolution.[20] Very recently, a porous organic push−pull polymer exhibited visible-light-induced hydrogen production from water when prepared as a composite with titanium dioxide.[21] Again, these systems all required the addition of a platinum cocatalyst.

A well-known advantage of organic polymers is that copolymers can be produced over a continuous range of monomer compositions, thus achieving systematic control over physical properties. This continuous tunability is distinct, for example, from that of crystalline inorganic solids, which often

Received: November 10, 2014
Revised: January 19, 2015
Accepted: February 3, 2015
Published: February 3, 2015

DOI: 10.1021/ja511552k
J. Am. Chem. Soc. 2015, 137, 3265−3270

exist as discrete phases with specific physical properties. For example, we demonstrated the fine-tuning of pore size in conjugated microporous polymers (CMPs) by statistical copolymerization.[22] Others showed that the fluorescence of microporous polymers can be varied by copolymerization strategies.[23] Copolymerization was also used to prepare polymers with tunable gas sorption properties.[24] Of particular relevance here, we were able to tune the optical gap for pyrene-based CMPs by statistical copolymerization.[25]

RESULTS AND DISCUSSION

We now report the synthesis of a library of CMP networks via statistical copolymerization and show that the adsorption/emission spectra, and hence the optical gap, can be tuned over a wide range in a continuous fashion. These polymer networks exhibit high levels of porosity of up to 1700 $m^2 g^{-1}$, and they can be used, without the addition of additional metal cocatalysts or photosensitizers, for the photocatalytic generation of hydrogen from water in the presence of a sacrificial electron donor. The materials are stable for several catalytic cycles without any obvious photodegradation. Some copolymers are exclusively active under visible light, rather than UV irradiation, which we believe is unique for organic photocatalysts.

Fifteen polymer networks were synthesized using Pd(0)-catalyzed Suzuki–Miyaura polycondensation[26] of 1,4-benzene diboronic acid (**1**) and/or 1,3,6,8-tetraboronic pinacol ester of pyrene (**3**) and/or 1,2,4,5-tetrabromobenzene (**2**) and/or 1,3,6,8-tetrabromopyrene (**4**) (Figure 1, Table 1).

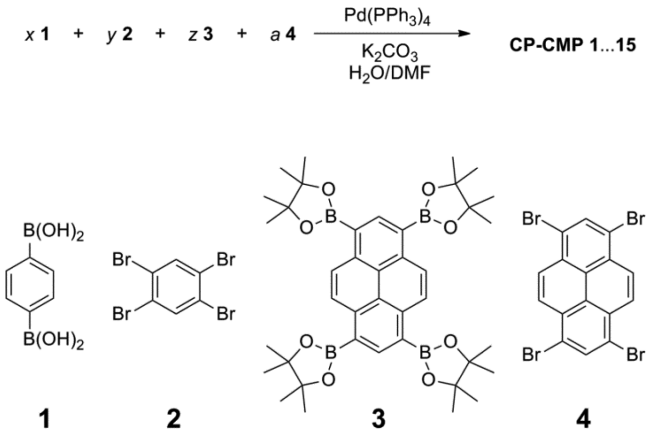

Figure 1. Synthesis of conjugated copolymer photocatalysts. Suzuki–Miyaura polycondensation produced a library of statistical copolymers with varying ratios of benzene and pyrene (Table 1).

All of the polymers are insoluble in organic solvents, and they were characterized by FT-IR spectroscopy and elemental analysis (Experimental Section, Supporting Information). Thermogravimetric analysis indicated that the polymers are thermally stable in air up to 300 °C (Figures S-4 and 5). Powder X-ray diffraction showed that all materials are amorphous. The polymers were porous to nitrogen at 77 K and give rise to type I sorption isotherms, indicating microporosity (pores < 2 nm, Figures S-6–10). The apparent Brunauer–Emmett–Teller (SA_{BET}) surface areas range from 600 to 1700 $m^2 g^{-1}$ (Table 1). Polymers CP-CMP1[27] and CP-CMP10[25,28] were both synthesized previously; all other networks in the series are first reported here. CP-CMP15 has the same nominal structure as our earlier polypyrene network,[25] but the synthetic protocol is different (Suzuki–Miyaura coupling instead of Yamamoto coupling). As a result, the absorption onset and the photoluminescence maximum for CP-CMP15 are both blue-shifted, suggesting that the polymer microstructure obtained using the Suzuki–Miyaura protocol is subtly different. The UV–visible reflectance spectra (Figure 2a) show a redshift in the optical absorption onset (optical gap) from 420 to 640 nm with an increase of pyrene content when going from CP-CMP1 to CP-CMP15. These data show that it is possible to fine-tune the optical properties of the CMP networks, and hence the optical gap (Table 2), over a broad range by adjusting the molar ratio of the monomers (Figure 2, top).

Table 1. Monomer Feed Ratios for the Copolymerization Reactions and Apparent Brunauer–Emmett–Teller Surface Areas of the Copolymers[a]

	relative molar monomer ratio				
copolymer	**1**	**2**	**3**	**4**	SA_{BET} ($m^2 g^{-1}$)[b]
CP-CMP1	2	1	0	0	597
CP-CMP2	2	0.99	0	0.01	682
CP-CMP3	2	0.95	0	0.05	710
CP-CMP4	2	0.90	0	0.10	684
CP-CMP5	2	0.80	0	0.20	734
CP-CMP6	2	0.60	0	0.40	726
CP-CMP7	2	0.50	0	0.50	839
CP-CMP8	2	0.40	0	0.60	1056
CP-CMP9	2	0.20	0	0.80	762
CP-CMP10	2	0	0	1	995
CP-CMP11	1.9	0	0.05	1	770
CP-CMP12	1.6	0	0.2	1	957
CP-CMP13	1	0	0.5	1	1710
CP-CMP14	0.4	0	0.8	1	1525
CP-CMP15	0	0	1	1	1218

[a]The structures of monomers **1**–**4** are shown in Figure 1. [b]Apparent BET surface area, SA_{BET}, is calculated from the N_2 adsorption isotherm.

Time-dependent density functional theory (TD-DFT) cluster calculations (Experimental Section, Supporting Information), using an approach reported previously,[29] suggest that the redshift in the UV–visible spectra with increasing pyrene incorporation is driven by a change in the character of the orbitals contributing to the excitations responsible for the optical gap. The highest occupied molecular orbital (HOMO) of a pyrene-containing system lies higher in energy than its phenylene equivalent. Equally, the lowest unoccupied molecular orbital (LUMO) of a pyrene-containing system lies lower in energy than its phenylene equivalent. Hence, upon increasing incorporation of pyrene, the low-energy excitations are dominated by pyrene contributions, and the optical gap shifts to higher wavelengths.

The photoluminescence spectrum for CP-CMP1, which contains no pyrene, is blue, with a maximum characteristic emission at 445 nm.[27] By contrast, the emission for the copolymers with pyrene units (CP-CMP2 through CP-CMP10) show a gradual redshift from a bluish-green emission at 465 nm (CP-CMP2) to a saturated green-yellow emission at 534 nm (CP-CMP10), and further to a red emission at 588 nm for CP-CMP15 (Figure 2b). We suggested before[29] that pyrene CMPs contain cyclic structures, or rings, and that ring-strain manifests itself as a redshift in the emission spectrum. Recently, Colina and co-workers[30] independently came to the same conclusions about the topology and strained nature of pyrene CMPs in their structural modeling work. Hence, the gradual redshift can probably be explained, as is the shift in the optical

DOI: 10.1021/ja511552k
J. Am. Chem. Soc. 2015, 137, 3265–3270

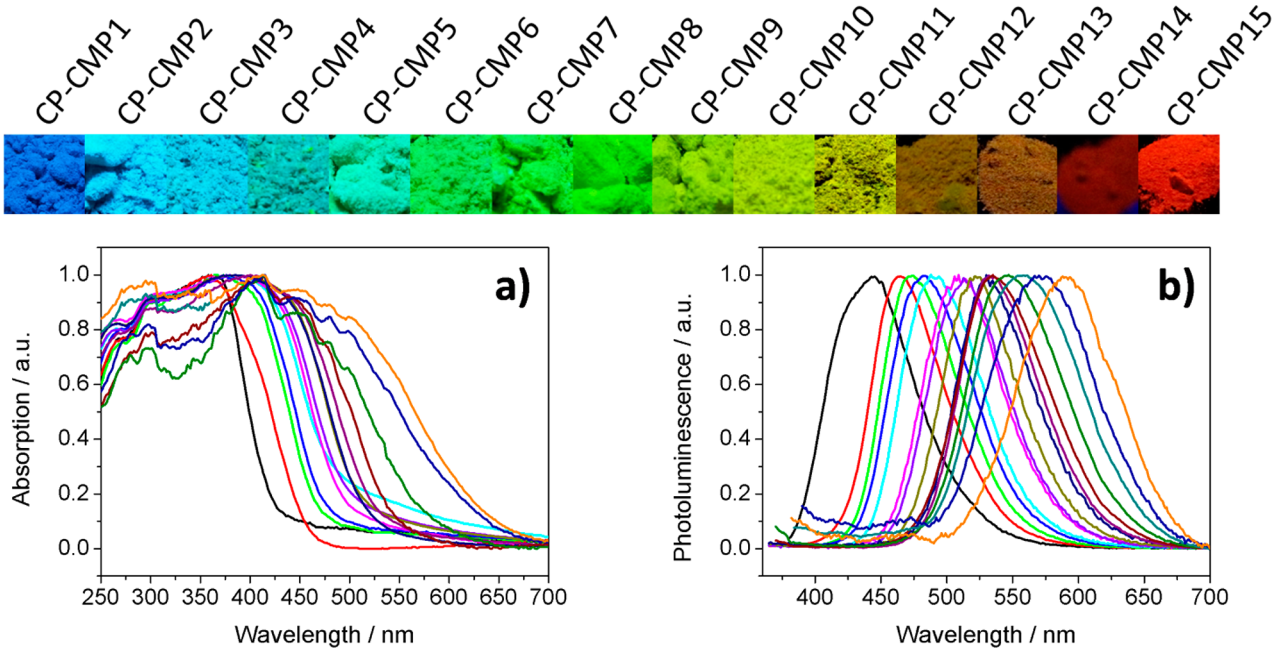

Figure 2. Statistical copolymerization allows continuous tuning of the photophysical properties of the photocatalysts. (top) Photographs of the 15 copolymers (CP-CMP1−15), imaged under irradiation with UV light ($\lambda_{excitation}$ = 365 nm); (a) UV−visible absorption spectra of the copolymers measured in the solid state (intensities normalized); (b) photoluminescence spectra of the copolymers, also measured in the solid state ($\lambda_{excitation}$ = 360 nm) and also normalized. (Absolute quantum yields can be found in the Table S-1.) A systematic redshift is observed as the pyrene monomer incorporation is increased.

Table 2. Photophysical Properties and Hydrogen Evolution Rates for the Polymer Photocatalysts

copolymer	λ_{em} (nm)[a]	optical gap (eV)[b]	total H_2 evolved (μmol)[c]	H_2 evolution rate (μmol h^{-1})[c]
CP-CMP1	445	2.95	5	1.0 ± 0.1
CP-CMP2	465	2.69	8	1.4 ± 0.1
CP-CMP3	474	2.61	11	1.8 ± 0.2
CP-CMP4	483	2.54	14	2.4 ± 0.1
CP-CMP5	498	2.53	17	3.0 ± 0.2
CP-CMP6	512	2.50	15	2.6 ± 0.2
CP-CMP7	517	2.47	17	2.9 ± 0.2
CP-CMP8	523	2.42	35	6.0 ± 0.6
CP-CMP9	528	2.38	69	10.9 ± 0.1
CP-CMP10	534	2.33	100	17.4 ± 0.9
CP-CMP11	535	2.24	11	2.0 ± 0.2
CP-CMP12	547	2.10	8	1.4 ± 0.2
CP-CMP13	558	2.07	6	1.0 ± 0.1
CP-CMP14	566	1.96	<0.5	<0.1
CP-CMP15	588	1.94	<1	0.2 ± <0.1

[a]Photoluminescent emission peak of polymer recorded in the solid state. [b]Calculated from the onset of the absorption spectrum; see discussion in the computational section of the Experimental Section, Supporting Information. [c]Reaction conditions: 100 mg polymer was suspended in 100 mL diethylamine/water solution (20 vol %) and irradiated by a 300 W Xe lamp (λ > 420 nm visible filter) for 6 h.

gap, by the incorporation of the pyrene chromophore itself, coupled with an increase in ring-strain down the copolymer series, especially beyond CP-CMP10 (Experimental Section, Supporting Information).

Photocatalytic hydrogen-evolution experiments were carried out with these CMPs in the presence of a sacrificial electron donor. Unlike for most previously reported polymer systems, diethylamine and not triethanolamine was selected because it showed the highest photocatalytic activity among a range of sacrificial reagents tested (Figure S-19). This might be due to better wettability or swelling of the polymer network in the water/diethylamine mixture. For CP-CMP10, swelling of the polymer network in the presence of solvents has been reported.[27]

All of the CMPs showed steady hydrogen production under illumination with visible light (λ > 420 nm, Table 2), with a gradual increase in the hydrogen evolution rate from CP-CMP1 to CP-CMP10, that is, as the optical gap of the polymer decreased. However, for polymers with even smaller optical gaps (i.e., CP-CMP11 through CP-CMP15), a sudden drop in the photocatalytic performance was observed (Figure 3).

The amounts of polymer used have not been optimized, and therefore all experiments were performed using either 100 mg or

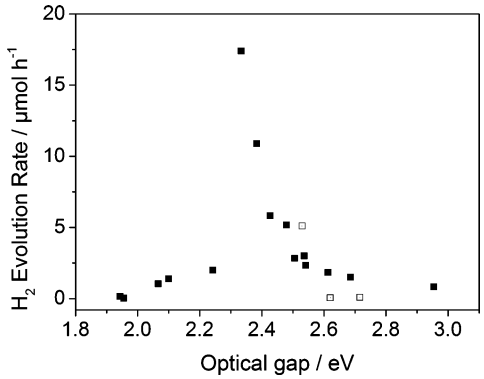

Figure 3. Rate of photocatalytic hydrogen production can be correlated with the optical gap in the polymers. Data shown for networks CP-CMP1−15 (black squares) and analogous linear polymers (discussed below), P16−18 (open squares); all measurements relate to 100 mg catalyst in water containing 20 vol % diethylamine as an electron donor under filtered, visible irradiation (λ > 420 nm, E < 2.95 eV).

DOI: 10.1021/ja511552k
J. Am. Chem. Soc. 2015, 137, 3265−3270

25 mg of catalyst with a fixed ratio of the catalyst amount to the volume of water/sacrificial reagent. For comparison, commercial graphitic carbon nitride and poly(*para*-phenylene) were tested with sacrificial reagents and cocatalysts previously employed in literature, using exactly the same setup as the polymers in this study (Experimental Section, Supporting Information).

TD-DFT cluster calculations[31,32] (Experimental Section, Supporting Information) suggested that these CMP materials should have a significant thermodynamic driving force (2−3 V) for the proton reduction half-reaction. As the optical gap is red-shifted in the series of CP-CMP1 to CP-CMP15, photons in a larger part of the visible spectrum are able to generate electrons that can reduce protons. Hence, one might reasonably expect that the rate of hydrogen production under visible light would increase down the series; indeed, theory agrees with the experiment for the series from CP-CMP1 to CP-CMP10. The dramatic drop in hydrogen production for polymers in the series beyond CP-CMP10 (Figure 3) suggests that dark, nonradiative electron−hole recombination in the pyrene-rich materials might become dominant, thus losing most electrons through recombination.

An alternative, kinetic explanation for the peak hydrogen production in CP-CMP10 is that the barrier for electron-transfer between the polymers and the protons increases with increasing pyrene content, thus reducing the amount of hydrogen evolved. We are not at this point able to distinguish between these explanations.

A typical time course for hydrogen production using CP-CMP10 catalyst under visible-light irradiation (λ > 420 nm) is shown in Figure 4a. The reaction was allowed to proceed for a total of 24 h with intermittent degassing of the reaction mixture every 6 h. Continuous hydrogen evolution was observed over the entire time course, even when the reaction was continued for a total of more than 100 h, without significant decline in activity (Figure S-20). The total amount of hydrogen evolved is equal to four times the amount of catalyst employed, indicating that the reaction proceeds photocatalytically. Furthermore, FT-IR, UV−vis, and photoluminescence spectra of the polymer network before and after the reaction showed no obvious signs of photodegradation, and the surface area of the catalyst is also retained (Figures S-21−23). Finally, control experiments showed that no reaction occurs in the dark at room temperature or 45 °C. No hydrogen evolution was observed in the absence of the polymer or when using pure diethylamine without water.

Unlike most examples in the literature, we added no additional noble metal cocatalysts to catalyze the hydrogen evolution. The polymers were, however, prepared via palladium-catalyzed Suzuki−Miyaura reactions. We therefore hypothesized that residual palladium metal in the polymers might assist in catalyzing the proton reduction. On measuring the residual metal contents, CP-CMP10 was found to contain a smaller amount of residual palladium than many of the other polymers in the series (0.42 wt %), despite displaying the highest rate of hydrogen evolution (Figure S-24). This suggests that residual metal is not the sole cause of the maximum hydrogen evolution activity in CP-CMP10. Likewise, when CP-CMP15 was synthesized again using a palladium-free Yamamoto protocol (CP-CMP15Y, Figure S-38), equivalent photocatalytic performance was observed (0.2 μmol h^{-1}) compared to the network synthesized using Suzuki−Miyaura polycondensation.[24] None of these results suggest that residual palladium has a significant effect on the rate of hydrogen evolution, but this does not eliminate the possibility that it plays a role in CMP-CMP10 and

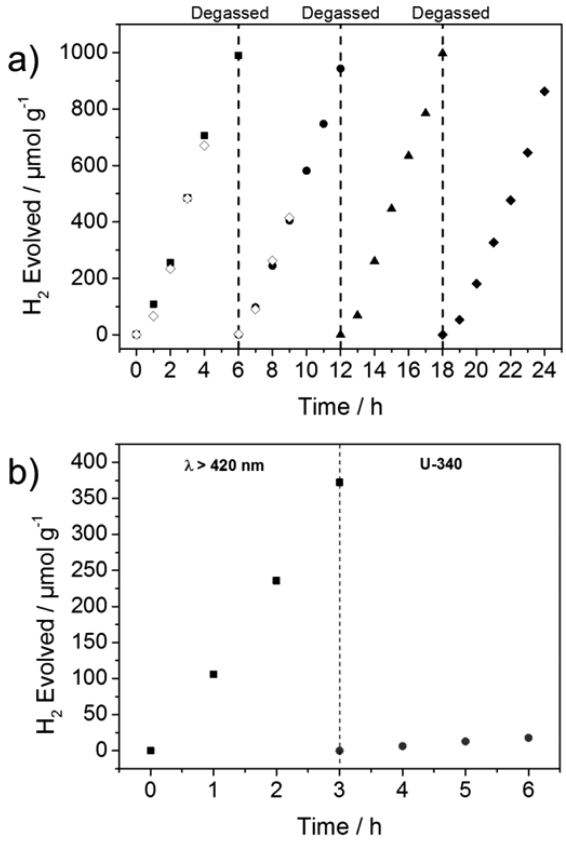

Figure 4. Photocatalytic hydrogen evolution is repeatable over multiple cycles and is mainly caused by visible light, not by UV irradiation. (a) Time course of hydrogen production for CP-CMP10 (100 mg) from water containing 20 vol % diethylamine as an electron donor under visible light (λ > 420 nm, black symbols). The reaction was degassed every 6 h (dashed line). Open diamonds represent an experiment where a suspension of CP-CMP10 (25 mg) was treated with carbon monoxide before the experiment. (b) Time course of H_2 production for CP-CMP10 (100 mg) under visible light (λ > 420 nm). The reaction was then degassed and continued under UV light (U-340 filter), whereupon the rate of H_2 evolution is almost 30 times lower.

the other more active photocatalysts. As a direct control experiment, a palladium-free equivalent of CP-CMP10 was prepared (CP-CMP10Y), again using the nickel-catalyzed Yamamoto protocol. However, in this case, the optical properties of CP-CMP10Y were markedly different from those of the Suzuki−Miyaura product, CP-CMP10, and a much lower rate of hydrogen evolution was observed for CP-CMP10Y (0.3 μmol h^{-1}, Figure S-39). This low activity could be rationalized by the optical gap for CP-CMP10Y (2.04 eV; c.f., Figure 3), and this again illustrates that polymer microstructure can affect absorption/emission spectra. It is unclear, therefore, whether the large drop in photocatalytic activity in CP-CMP10Y with respect to CP-CMP10 is a result of the absence of palladium or its optical properties or both. We note that CP-CMP14 and CP-CMP15 have optical gaps similar to that of CP-CMP10Y and equally low photocatalytic activities (Figure 3), despite having measurable palladium contents (0.73 and 0.40 wt %). However, CP-CMP14 and CP-CMP15 are also significantly more pyrene-rich than CP-CMP10Y, and this might lead to subtle microstructural differences, such as ring formation, that could influence charge separation and charge transport. As such, the photocatalytic activity for the polymers may not be a simple function of optical gap and palladium content alone.

DOI: 10.1021/ja511552k
J. Am. Chem. Soc. 2015, 137, 3265−3270

To further probe the effect of metal cocatalysts, we tested the hydrogen evolution performance for CP-CMP10 loaded postsynthesis with platinum, using the widely used method of photocatalytic deposition from H_2PtCl_6.[6,12,19,20,33] However, attempted loading of CP-CMP10 with 3 wt % platinum seems to be inefficient, and the system showed no improvement in hydrogen evolution rate (Figure S-42).[34] TEM images seem to indicate that no Pt nanoparticles have been formed during the deposition of Pt on CP-CMP10. The synthesized sample and the Pt-loaded sample seem to contain the same amount of dense metal particles that are probably the aforementioned Pd nanoparticles (Figure S-43).[35] Overall, we see no correlation between photocatalytic activity and metal loading for the polymers in this series (Figure S-24). Hence, it appears that the polymers are effective photocatalysts without any additional metal cocatalyst and that the rate of hydrogen evolution correlates more strongly with the optical gap than with the residual palladium content. Finally, a carbon monoxide poisoning experiment (Figure 4a) did not result in any change to the catalytic activity.

Batch-to-batch and repeat measurements on a sample of CP-CMP10 indicated an average hydrogen evolution rate of 17.4 ± 0.9 μmol h^{-1}. The value is significantly higher than that observed for poly(azomethine) networks loaded with 3 wt % Pt cocatalyst (0.7 μmol h^{-1})[19] and graphitic carbon nitride with 3 wt % Pt cocatalyst (6.5 and 10.7 μmol h^{-1}).[6,9,34] The rate is similar to those of other recent reports for carbon nitrides,[8,16] although lower than some reported for mesoporous carbon nitrides[10] and related materials.[12,20] Direct comparison between different data sets, however, is difficult because of variations in the reaction setup;[36] indeed, the reported values for carbon nitride itself vary significantly from study to study.[6,10,12,34] We note again, however, that other reports involve the postsynthesis addition of around 3 wt % metal cocatalysts to achieve good hydrogen evolution rates.[34]

Perhaps the most important feature of our polymers is their photocatalytic activity under visible light. Graphitic carbon nitride is also active under visible light (>420 nm), but it is far more active under UV irradiation.[9] This presents a challenge for the effective utilization of the natural solar spectrum, where only 3% or so of the available energy is in the UV range. By contrast, our polymers are mainly active in the visible range. For CP-CMP10, replacement of the >420 nm filter with a 710−315 nm filter resulted in a very similar rate of hydrogen production, indicating that UV light with wavelengths lower than 420 nm contributes little to the photocatalysis. Moreover, by using a filter that only transmits UV light (U-340, 270−400 nm, see Figure S44 for transmission characteristics), hydrogen was evolved at a rate of just 0.6 μmol h^{-1} (Figure 4b). Hence, CP-CMP10 appears to be a true visible light photocatalyst. To our knowledge, this visible light bias is unique among organic photocatalysts for hydrogen evolution.

We also performed studies on oxygen evolution to probe whether full water splitting is possible with CP-CMP1 and CP-CMP10. However, no O_2 was detected under the conditions used. (TD-)DFT-calculations also show that the system lacks driving-force for oxidation of water (Experimental Section, Supporting Information)

Three linear copolymer analogues of CP-CMP10 were synthesized to study the effect of polymer nanostructure on optical properties and on photocatalytic activity (Figure 5). Polymer P16 contains, exclusively, 1,3-substituted pyrene monomer units, whereas P17 contains only 1,6-linked monomers; P18 has, as in CP-CMP10, a statistical mixture of both 1,3- and 1,6-substituents.

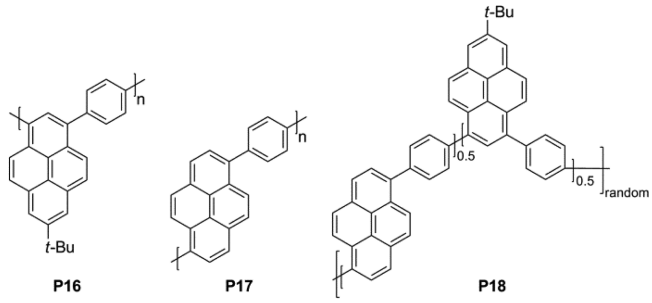

Figure 5. Structures of linear copolymer analogues of the CP-CMP10 network.

The optical gap for P16 is blue-shifted by 74 nm with respect to CP-CMP10; likewise, P17 is blue-shifted by 41 nm (Figure S-14). The emission maxima are also blue-shifted by 69 and 35 nm, respectively, for P16 and P17. The optical gap of the statistical copolymer, P18, lies between those of P16 and P17. We believe that these absorption shifts are further evidence for structural elements, such as rings,[29] that can form in network CP-CMP10 but not in the linear three polymers.

Polymers P16 and P18 showed modest BET surface areas that were comparable with other intrinsically porous linear CMPs,[37] whereas P17 was effectively nonporous, perhaps suggesting that the 1,3-pyrene linkages contribute to contortion in the polymer chains, and hence inefficient packing and porosity. When tested as photocatalysts, P16 produced a negligible amount of hydrogen under visible light (>420 nm). P17 and P18 have average hydrogen evolution rates of 5.0 ± 0.4 and 3.8 ± 3 μmol h^{-1}, respectively, under visible light, but when the >420 filter was replaced with a 315−710 nm filter, significantly higher rates of 11.7 ± 1.1 and 5.7 ± 0.5 μmol h^{-1}, respectively, were observed. The changes in photocatalytic activity with respect to network CP-CMP10 can be explained by the differences in the absorption profiles of the various polymers. For both CP-CMP10 and P17, the use of filters that remove light at wavelengths higher than the polymer absorption maximum significantly reduces the photocatalytic performance (Figures S-52 and 53).

The good photocatalytic activity of P17 under combined UV and visible light indicates that a low BET surface area (13 m^2 g^{-1}) is not necessarily a limiting factor for the performance of these polymers. In fact, no direct correlation between photocatalytic performance and surface area was found for this series of photocatalysts (Figure S-55). In general, however, the ability to introduce a large, distributed interface with water should be an advantage in designing improved organophotocatalysts, both in terms of optimizing mass transport and in allowing strategies such as the introduction of dopants in the micropores. High surface areas should also be an advantage in other heterogeneous photocatalysis applications.[38,39]

■ CONCLUSIONS

The optical gap in a series of microporous copolymers was fine-tuned over a broad range (1.94−2.95 eV) by varying monomer composition. This optical gap determines the efficiency of the copolymers as photocatalysts for hydrogen evolution. Unlike most hydrogen-producing photocatalysts, certain copolymers are active under visible light, and UV light contributes little to the photocatalytic activity, possibly because higher-energy excited states are diverted into pathways that are not suitable for

DOI: 10.1021/ja511552k
J. Am. Chem. Soc. 2015, 137, 3265−3270

hydrogen generation. These polymers do not require the deposition of an additional metal cocatalyst and deliberate "poisoning" of the polymer with carbon monoxide does not affect the H_2 evolution rate. Our modular chemical strategy has parallels with the chemical synthesis of graphene nanomaterials,[40] and synthetic control over electronic structure and microporosity should facilitate the design of improved photocatalysts for overall water splitting in the future.

■ ASSOCIATED CONTENT

Supporting Information

Full synthetic details and analysis for the polymers, TGA, FT-IR, gas sorption, UV/PL spectra, TEM data, further photocatalysis data, and (TD-)DFT calculations. This material is available free of charge via the Internet at http://pubs.acs.org.

■ AUTHOR INFORMATION

Corresponding Authors

*d.j.adams@liverpool.ac.uk
*aicooper@liverpool.ac.uk

Notes

The authors declare no competing financial interest.

■ ACKNOWLEDGMENTS

We thank EPSRC (EP/C511794/1) for funding. M.A.Z. acknowledges EPSRC for a fellowship (EP/I004424/1). We thank F. Armstrong, M. Bojdys, C. Butchosa, A. Cowan, J. Walsh, G. Cheng, and B. Kiss for helpful discussions. T. Hasell is acknowledged for help with TGA measurements and with SEM. We acknowledge computational time on HECToR/ARCHER, the United Kingdom's national high-performance computing (HPC) service, via our membership of the United Kingdom's HPC Materials Chemistry Consortium, which is funded by EPSRC grants EP/F067496/1 and EP/L000202/1, and also the EPSRC United Kingdom National Service for Computational Chemistry Software (NSCCS) at Imperial College London.

■ REFERENCES

(1) Chen, X.; Shen, S.; Guo, L.; Mao, S. S. *Chem. Rev.* **2010**, *110*, 6503.
(2) Kudo, A.; Miseki, Y. *Chem. Soc. Rev.* **2009**, *38*, 253.
(3) Yang, L.; Zhou, H.; Fan, T.; Zhang, D. *Phys. Chem. Chem. Phys.* **2014**, *16*, 6810.
(4) Yanagida, S.; Kabumoto, A.; Mizumoto, K.; Pac, C.; Yoshino, K. *J. Chem. Soc., Chem. Commun.* **1985**, 474.
(5) Shibata, T.; Kabumoto, A.; Shiragami, T.; Ishitani, O.; Pac, C.; Yanagida, S. *J. Phys. Chem.* **1990**, *94*, 2068.
(6) Wang, X.; Maeda, K.; Thomas, A.; Takanabe, K.; Xin, G.; Carlsson, J. M.; Domen, K.; Antonietti, M. *Nat. Mater.* **2009**, *8*, 76.
(7) Zhang, G.; Wang, X. *J. Catal.* **2013**, *307*, 246.
(8) Martha, S.; Nashim, A.; Parida, K. M. *J. Mater. Chem. A* **2013**, *1*, 7816.
(9) Zhang, J.; Chen, X.; Takanabe, K.; Maeda, K.; Domen, K.; Epping, J. D.; Fu, X.; Antonietti, M.; Wang, X. *Angew. Chem., Int. Ed.* **2010**, *49*, 441.
(10) Wang, X.; Maeda, K.; Chen, X.; Takanabe, K.; Domen, K.; Hou, Y.; Fu, X.; Antonietti, M. *J. Am. Chem. Soc.* **2009**, *131*, 1680.
(11) Kailasam, K.; Epping, J. D.; Thomas, A.; Losse, S.; Junge, H. *Energy Environ. Sci.* **2011**, *4*, 4668.
(12) Schwinghammer, K.; Tuffy, B.; Mesch, M. B.; Wirnhier, E.; Martineau, C.; Taulelle, F.; Schnick, W.; Senker, J.; Lotsch, B. V. *Angew. Chem., Int. Ed.* **2013**, *52*, 2435.
(13) Kailasam, K.; Schmidt, J.; Bildirir, H.; Zhang, G.; Blechert, S.; Wang, X.; Thomas, A. *Macromol. Rapid Commun.* **2013**, *34*, 1008.
(14) Jiang, D.; Chen, L.; Xie, J.; Chen, M. *Dalton Trans.* **2014**, *43*, 4878.
(15) Sui, Y.; Liu, J.; Zhang, Y.; Tian, X.; Chen, W. *Nanoscale* **2013**, *5*, 9150.
(16) Wang, X. L.; Fang, W. Q.; Yang, S.; Liu, P.; Zhao, H.; Yang, H. G. *RSC Adv.* **2014**, *4*, 10676.
(17) Hollmann, D.; Karnahl, M.; Tschierlei, S.; Kailasam, K.; Schneider, M.; Radnik, J.; Grabow, K.; Bentrup, U.; Junge, H.; Beller, M.; Lochbrunner, S.; Thomas, A.; Brückner, A. *Chem. Mater.* **2014**, *26*, 1727.
(18) Martin, D. J.; Qiu, K.; Shevlin, S. A.; Handoko, A. D.; Chen, X.; Guo, Z.; Tang, J. *Angew. Chem., Int. Ed.* **2014**, *53*, 9240.
(19) Schwab, M. G.; Hamburger, M.; Feng, X.; Shu, J.; Spiess, H. W.; Wang, X.; Antonietti, M.; Mullen, K. *Chem. Commun.* **2010**, *46*, 8932.
(20) Stegbauer, L.; Schwinghammer, K.; Lotsch, B. V. *Chem. Sci.* **2014**, *5*, 2789.
(21) Park, J. H.; Ko, K. C.; Park, N.; Shin, H.-W.; Kim, E.; Kang, N.; Hong Ko, J.; Lee, S. M.; Kim, H. J.; Ahn, T. K.; Lee, J. Y.; Son, S. U. *J. Mater. Chem. A* **2014**, *2*, 7656.
(22) Jiang, J.-X.; Su, F.; Trewin, A.; Wood, C. D.; Niu, H.; Jones, J. T. A.; Khimyak, Y. Z.; Cooper, A. I. *J. Am. Chem. Soc.* **2008**, *130*, 7710.
(23) Brandt, J.; Schmidt, J.; Thomas, A.; Epping, J. D.; Weber, J. *Polymer Chem.* **2011**, *2*, 1950.
(24) Pei, C.; Ben, T.; Li, Y.; Qiu, S. L. *Chem. Commun.* **2014**, *50*, 6134.
(25) Jiang, J.-X.; Trewin, A.; Adams, D. J.; Cooper, A. I. *Chem. Sci.* **2011**, *2*, 1777.
(26) Weber, J.; Thomas, A. *J. Am. Chem. Soc.* **2008**, *130*, 6334.
(27) Chen, L.; Honsho, Y.; Seki, S.; Jiang, D. *J. Am. Chem. Soc.* **2010**, *132*, 6742.
(28) Rao, K. V.; Mohapatra, S.; Maji, T. K.; George, S. J. *Chem.—Eur. J.* **2012**, *18*, 4505.
(29) Zwijnenburg, M. A.; Cheng, G.; McDonald, T. O.; Jelfs, K. E.; Jiang, J.-X.; Ren, S.; Hasell, T.; Blanc, F.; Cooper, A. I.; Adams, D. J. *Macromolecules* **2013**, *46*, 7696.
(30) Abbott, L. J.; Colina, C. M. *J. Chem. Eng. Data* **2014**, *59*, 3177.
(31) Guiglion, P.; Butchosa, C.; Zwijnenburg, M. A. *J. Mater. Chem. A* **2014**, *2*, 11996.
(32) Butchosa, C.; Guiglion, P.; Zwijnenburg, M. A. *J. Phys. Chem. C* **2014**, *118*, 24833.
(33) Graphitic carbon nitride tested on our specific experimental setup gave a hydrogen production rate of 19.0 ± 0.4 μmol h^{-1} under visible light irradiation with 3 wt% Pt loading (Experimental Section, Supporting Information).
(34) Wang, Y.; Di, Y.; Antonietti, M.; Li, H.; Chen, X.; Wang, X. *Chem. Mater.* **2010**, *22*, 5119.
(35) Experiments were also performed using $RuCl_3$ and $RhCl_3{\cdot}H_2O$ as cocatalysts. However, these experiments did not result in any improvement of the hydrogen production rate, but rather lowered the rate significantly.
(36) Schwarze, M.; Stellmach, D.; Schroder, M.; Kailasam, K.; Reske, R.; Thomas, A.; Schomacker, R. *Phys. Chem. Chem. Phys.* **2013**, *15*, 3466.
(37) Cheng, G.; Bonillo, B.; Sprick, R. S.; Adams, D. J.; Hasell, T.; Cooper, A. I. *Adv. Funct. Mater.* **2014**, *24*, 5219.
(38) Kaur, P.; Hupp, J. T.; Nguyen, S. T. *ACS Catal.* **2011**, *1*, 819.
(39) Xie, Z.; Wang, C.; de Krafft, K. E.; Lin, W. *J. Am. Chem. Soc.* **2011**, *133*, 2056.
(40) Cai, J.; Ruffieux, P.; Jaafar, R.; Bieri, M.; Braun, T.; Blankenburg, S.; Muoth, M.; Seitsonen, A. P.; Saleh, M.; Feng, X.; Mullen, K.; Fasel, R. *Nature* **2010**, *466*, 470.

DOI: 10.1021/ja511552k
J. Am. Chem. Soc. 2015, 137, 3265−3270